

# Photoinduced Electron-Transfer Reactions of Plastocyanin with the Triplet State of Zinc Myoglobin and with the Zinc Myoglobin Cation Radical. Protein–Protein Orientation in the Absence of Strong Electrostatic Interactions

Jun Cheng, Jian S. Zhou, and Nenad M. Kostić\*

Department of Chemistry, Iowa State University, Ames, Iowa 50011

Received August 4, 1993\*

Various redox properties and electron-transfer reactions of myoglobin have been studied, but very few of these studies have dealt with reactions between myoglobin and other redox proteins. We report kinetics of two such photoinduced bimolecular reactions—reduction of cupriplastocyanin by the triplet state of zinc myoglobin (the forward reaction) and oxidation of cuproplastocyanin by the cation radical of zinc myoglobin (the back reaction). A widely-used version of Debye–Hückel theory reproduces the dependence on ionic strength of the forward reaction but not of the back reaction. Dependence on ionic strength of the forward rate constant is treated by van Leeuwen theory, which recognizes monopole–monopole, monopole–dipole, and dipole–dipole interactions between the protein molecules. Fitting of the kinetic results reveals the overall protein–protein orientation for electron transfer. Myoglobin lacks distinct charged patches on its surface, its net charge is nearly zero, and its heme is buried. In the absence of significant electrostatic attraction to cupriplastocyanin, an area near the heme crevice in zinc myoglobin seems to abut the electroneutral hydrophobic patch in plastocyanin, which is proximate to the copper atom. This finding is compared with our previous findings concerning zinc cytochrome *c*, which has a positively charged patch surrounding the exposed heme edge. In that case, strong electrostatic attraction keeps the exposed heme near the acidic patch, which is remote from the copper atom. Protein–protein orientation for electron transfer depends on an interplay between electrostatic interactions and donor–acceptor coupling, among other factors.

## Introduction

**Redox Reactions of Metalloproteins.** Because metalloproteins are essential to biological oxidoreduction processes, electron-transfer reactions of these proteins are being much studied.<sup>1–9</sup> One of the factors governing selectivity of these reactions at the molecular level is protein–protein orientation. Because charged groups in proteins can be unsymmetrically distributed, electrostatic interactions maintaining this orientation can be very anisotropic. Analysis of this anisotropy by kinetic methods can reveal protein–protein orientation in a reaction.

**Plastocyanin and Cytochromes.** The three-dimensional structure of plastocyanin in both oxidized and reduced states, designated pc(II) and pc(I), is known in detail.<sup>10</sup> This blue copper protein is notable for it contains on the surface two distinct patches through which it can exchange electrons with redox partners.<sup>11–13</sup> The negatively charged acidic patch is remote from the copper atom, whereas the electroneutral hydrophobic patch is proximate to this atom. Because both patches are made up of side chains in the protein strands that are ligated to the copper atom, both of them are well coupled electronically to the redox-active site.<sup>14</sup> The rate of electron transfer through proteins may be controlled

by the donor–acceptor distance,<sup>15</sup> or discrete paths through bonds may exist.<sup>16–18</sup> From either of these competing points of view, the proximate channel should permit much higher transfer rates than the remote channel.<sup>19,20</sup> That the actual rates are comparable has been attributed to the anisotropic covalency of the highest occupied molecular orbital of the copper site.<sup>19</sup> In the case of positively charged redox agents, electrostatic attraction to the remote patch may contribute to the efficacy of the remote channel.<sup>11,12</sup>

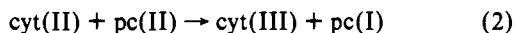
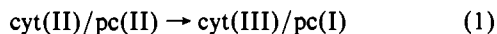
In our previous studies, plastocyanin was treated with cytochrome *c* (which is not a physiological partner),<sup>21,22</sup> with cytochrome *f* (which is),<sup>23,24</sup> and with cytochrome *c* derivatives reconstituted with zinc(II)<sup>25–30</sup> and tin(IV).<sup>30</sup> The first two proteins are both designated cyt, and the last two derivatives are designated Zn(cyt) and Sn(cyt). In each of them, the exposed heme edge is surrounded by lysine residues,<sup>31</sup> and this positively charged (basic) patch abuts the broad acidic patch as the electrostatic diprotein complexes cyt/pc, Zn(cyt)/pc, and Sn-

\* Abstract published in *Advance ACS Abstracts*, March 15, 1994.

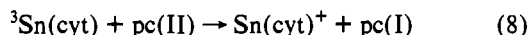
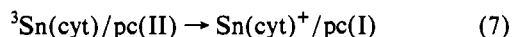
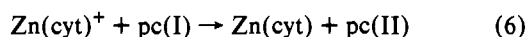
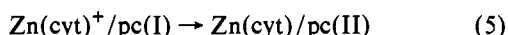
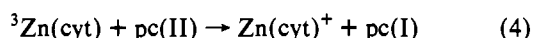
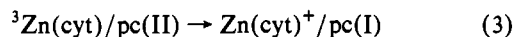
- (1) Hoffman, B. M.; Natan, M. J.; Nocek, J. M.; Wallin, S. A. *Struct. Bonding* **1991**, *75*, 86.
- (2) McLendon, G. *Struct. Bonding* **1991**, *75*, 160.
- (3) McLendon, G. *Met. Ions Biol. Syst.* **1991**, *27*, 183.
- (4) McLendon, G.; Hake, R. *Chem. Rev.* **1992**, *92*, 481.
- (5) Therien, M. J.; Chang, J.; Raphael, A. L.; Bowler, B. E.; Gray, H. B. *Struct. Bonding* **1991**, *75*, 110.
- (6) Winkler, J. R.; Gray, H. B. *Chem. Rev.* **1992**, *92*, 369.
- (7) Mauk, A. G. *Struct. Bonding* **1991**, *75*, 131.
- (8) Kostić, N. M. *Met. Ions Biol. Syst.* **1991**, *27*, 129.
- (9) Willie, A.; Stayton, P. S.; Sligar, S. G.; Durham, B.; Millett, F. *Biochemistry* **1992**, *31*, 7237.
- (10) Guss, J. M.; Freeman, H. C. *J. Mol. Biol.* **1983**, *169*, 521.
- (11) Sykes, A. G. *Struct. Bonding* **1991**, *75*, 177.
- (12) Sykes, A. G. *Adv. Inorg. Chem.* **1991**, *36*, 377.
- (13) Christensen, H. E. M.; Conrad, L. S.; Ulstrup, J.; Mikkelsen, K. V. *Met. Ions Biol. Syst.* **1991**, *27*, 57.
- (14) Betts, J. N.; Beratan, D. N.; Onuchic, J. N. *J. Am. Chem. Soc.* **1992**, *114*, 4043.

- (15) Moser, C. C.; Keske, J. M.; Warncke, K.; Farid, R. S.; Dutton, P. L. *Nature* **1992**, *355*, 796.
- (16) Beratan, D. N.; Onuchic, J. M.; Gray, H. B. *Met. Ions Biol. Syst.* **1991**, *27*, 97.
- (17) Wuttke, D. W.; Bjerrum, M. J.; Winkler, J. R.; Gray, H. B. *Science* **1992**, *256*, 1007.
- (18) Beratan, D. N.; Betts, J. N.; Onuchic, J. N. *Science* **1991**, *252*, 1285.
- (19) Lowery, M. D.; Guckert, J. A.; Gebhard, M. S.; Solomon, E. I. *J. Am. Chem. Soc.* **1993**, *115*, 3012.
- (20) Christensen, H. E. M.; Conrad, L. S.; Mikkelsen, K. V.; Nielsen, M. K.; Ulstrup, J. *Inorg. Chem.* **1990**, *29*, 2808.
- (21) Peerey, L. M.; Kostić, N. M. *Biochemistry* **1989**, *28*, 1861.
- (22) Peerey, L. M.; Brothers, H. M., II; Hazzard, J. T.; Tollin, G.; Kostić, N. M. *Biochemistry* **1991**, *30*, 9297.
- (23) Qin, L.; Kostić, N. M. *Biochemistry* **1992**, *31*, 5145.
- (24) Qin, L.; Kostić, N. M. *Biochemistry* **1993**, *32*, 6073.
- (25) Zhou, J. S.; Kostić, N. M. *J. Am. Chem. Soc.* **1991**, *113*, 6067.
- (26) Zhou, J. S.; Kostić, N. M. *J. Am. Chem. Soc.* **1991**, *113*, 7040.
- (27) Zhou, J. S.; Kostić, N. M. *J. Am. Chem. Soc.* **1992**, *114*, 3562.
- (28) Zhou, J. S.; Kostić, N. M. *The Spectrum* **1992**, *5* (2), 1.
- (29) Zhou, J. S.; Kostić, N. M. *Biochemistry* **1993**, *32*, 4539.
- (30) Zhou, J. S.; Kostić, N. M. *J. Am. Chem. Soc.* **1993**, *115*, 10796.
- (31) Moore, G. R.; Pettigrew, G. W. *Cytochromes c: Evolutionary, Structural and Physicochemical Aspects*; Springer-Verlag: Berlin, 1990.

(cyt)/pc are formed.<sup>32-34</sup> Studies in our laboratory and in others of the unimolecular reaction in eq 1<sup>21,22</sup> and of the bimolecular reaction in eq 2<sup>35,36</sup> showed that the weak reductants ferrocyto-



chrome *c* and ferrocytochrome *f*, which are both designated cyt-(II), reduce cupriplastocyanin from the acidic patch, but not from the initial binding site within this broad patch. Studies in our laboratory<sup>25-30</sup> of the corresponding reactions in eqs 3-8



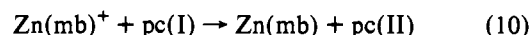
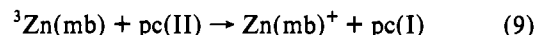
showed that the strong reductant zinc cytochrome *c* in the triplet state (<sup>3</sup>Zn(cyt)) can reduce cupriplastocyanin from the initial binding site, within the acidic patch, when rearrangement of the diprotein complex is prevented by noninvasive cross-linking. Even when the rearrangement does occur, within electrostatic complexes and in bimolecular reactions, the exposed heme edge does not seem to move away from the acidic patch. Dependence of the reaction rates on solvent viscosity revealed an interplay between the electron-transfer event and the rearrangement of the diprotein complexes such that the ground-state reaction in eq 1 is not gated, whereas the corresponding excited-state reactions in eqs 3 and 7 are gated. Equations 3, 4, and 7 represent so-called forward or excited-state reactions, whereas eqs 5, 6, and 8 represent so-called back or thermal reactions.

**Myoglobin as a Redox Protein.** Although this heme protein, designated mb, is not a physiological redox agent, its thorough structural characterization and its convenient properties made it suitable also for study of electron-transfer reactions with small redox agents.<sup>37-44</sup> Gray et al. have elegantly studied intraprotein reactions in myoglobin labeled with ruthenium complexes.<sup>45-53</sup>

- (32) Bagby, S.; Driscoll, P. C.; Goodall, K. G.; Redfield, C.; Hill, H. A. O. *Eur. J. Biochem.* **1990**, *188*, 413.  
 (33) Roberts, V. A.; Freeman, H. C.; Getzoff, E. D.; Olson, A. J.; Tainer, J. A. *J. Biol. Chem.* **1991**, *266*, 13431.  
 (34) Zhou, J. S.; Brothers, H. M., II; Nedderson, J. P.; Cotton, T. M.; Peerey, L. M.; Kostić, N. M. *Bioconjugate Chem.* **1992**, *3*, 382.  
 (35) Modi, S.; He, S.; Gray, J. C.; Bendall, D. S. *Biochim. Biophys. Acta* **1992**, *1101*, 64.  
 (36) Modi, S.; Nordling, M.; Lundberg, L. G.; Hansson, Ö; Bendall, D. S. *Biochim. Biophys. Acta* **1992**, *1102*, 85.  
 (37) Zemel, H.; Hoffman, B. M. *J. Am. Chem. Soc.* **1981**, *103*, 1192.  
 (38) Barboy, N.; Feitelson, J. *Biochemistry* **1987**, *26*, 3240.  
 (39) Barboy, N.; Feitelson, J. *Biochemistry* **1989**, *28*, 5450.  
 (40) Shosheva, A. C.; Christova, P. K.; Atanasov, B. P. *Biochim. Biophys. Acta* **1988**, *957*, 202.  
 (41) Aono, S.; Nemoto, S.; Okura, I. *Bull. Chem. Soc. Jpn.* **1992**, *65*, 591.  
 (42) Feitelson, J.; McLendon, G. *Biochemistry* **1991**, *30*, 5051.  
 (43) Tsukahara, K.; Asami, S. *Chem. Lett.* **1991**, 1337.  
 (44) Tsukahara, K.; Okada, M. *Chem. Lett.* **1992**, 1543.  
 (45) Crutchley, R. J.; Ellis, W. R., Jr.; Gray, H. B. *J. Am. Chem. Soc.* **1985**, *107*, 5002.  
 (46) Mayo, S. L.; Ellis, W. R., Jr.; Crutchley, R. J.; Gray, H. B. *Science* **1986**, *233*, 948.  
 (47) Lieber, C. M.; Karas, J. L.; Gray, H. B. *J. Am. Chem. Soc.* **1987**, *109*, 3778.  
 (48) Cowan, J. A.; Upmacis, R. K.; Beratan, D. N.; Onuchic, J. N.; Gray, H. B. *Ann. N.Y. Acad. Sci.* **1988**, *550*, 68.  
 (49) Karas, J. L.; Lieber, C. M.; Gray, H. B. *J. Am. Chem. Soc.* **1988**, *110*, 599.  
 (50) Axup, A. W.; Albin, M.; Mayo, S. L.; Crutchley, R. J.; Gray, H. B. *J. Am. Chem. Soc.* **1988**, *110*, 435.

We know of only two studies concerning reactions between myoglobin and redox proteins.<sup>54,55</sup> The ease of replacing heme with other metalloporphyrins makes myoglobin well suited for biophysical studies<sup>56-58</sup> and for studies of photoinduced electron-transfer reactions.<sup>49-53,59</sup> Very recent experimental work by Gray et al.<sup>53</sup> and theoretical work by Siddarth and Marcus<sup>60</sup> indicated that the electron carrier cytochrome *c* and the oxygen carrier myoglobin differ in the electronic coupling and in electron-transfer paths that they provide in redox reactions. This intriguing difference should be investigated more in protein-protein systems.<sup>61,62</sup> The present study may be the first one in which cytochrome *c* and myoglobin are compared in analogous reactions with another redox protein.

**Plastocyanin and Zinc Myoglobin.** Both zinc cytochrome *c* and zinc myoglobin are readily excited into the triplet state, designated <sup>3</sup>Zn(cyt) and <sup>3</sup>Zn(mb), but these two proteins differ otherwise. The heme group in cytochrome *c* is somewhat exposed, the protruding edge is surrounded by positively charged residues, and the protein as a whole bears a large positive charge in neutral solution. By contrast, the heme group in myoglobin is buried, the protein lacks charged patches on the surface, and its net charge is approximately zero in neutral solution (*pI* ≈ 7.0). Because <sup>3</sup>Zn(cyt) and <sup>3</sup>Zn(mb) have similar redox potentials (-0.80 to -0.90 V)<sup>51,63</sup> but different heme exposures and electrostatic properties, their reactions with plastocyanin (*E*<sup>o</sup> = +0.36 V) have similar driving force (ca. 1.2 eV) but may differ in protein-protein orientations. Here we study the forward reaction (eq 9) and the back reaction (eq 10) and apply van Leeuwen theory to



compare the protein-protein orientations in the analogous forward reactions in eqs 4 and 9. The results indicate that, in the absence of strong electrostatic interactions, plastocyanin uses its hydrophobic patch in electron-transfer reactions with heme proteins, especially if the heme is buried or only slightly exposed.

## Experimental Procedures

**Chemicals.** Mesoporphyrin IX dimethyl ester and myoglobins from sperm whale and horse heart were obtained from Sigma Chemical Co. Plastocyanin from French bean was isolated by standard methods<sup>64</sup> and purified repeatedly by gel-filtration chromatography and by anion-exchange chromatography, as described before.<sup>25,29</sup> The absorbance quotient *A*<sub>278</sub>/*A*<sub>597</sub> < 1.20 was achieved. Cuproplastocyanin, pc(I), was always prepared fresh by reduction with ascorbic acid, followed by removal of the reductant and of other small compounds by a Bio-Gel P-6 column. Concentration of cuproplastocyanin in stock solutions was determined by oxidizing an aliquot with an excess of K<sub>3</sub>[Fe(CN)<sub>6</sub>] and by spectrophotometric quantitation of cupriplastocyanin, for which ε<sub>597</sub> = 4500 M<sup>-1</sup> cm<sup>-1</sup>. Oxidation of cuproplastocyanin by air was not detected.

- (51) Cowan, J. A.; Gray, H. B. *Inorg. Chem.* **1989**, *28*, 2074.  
 (52) Gray, H. B. *Aldrichimica Acta* **1990**, *23*, 87.  
 (53) Casimiro, D. R.; Wong, L.-L.; Colón, J. L.; Zewert, T. E.; Richards, J. H.; Chang, I.-J.; Winkler, J. R.; Gray, H. B. *J. Am. Chem. Soc.* **1993**, *115*, 1485.  
 (54) Livingston, D. J.; McLachlan, S. J.; La Mar, G. N.; Brown, W. D. *J. Biol. Chem.* **1985**, *260*, 15699.  
 (55) Postnikova, G. B.; Tselikova, S. V.; Sivozhel, V. S. *Mol. Biol. (Engl. Transl.)* **1992**, *26*, 594.  
 (56) Papp, S.; Vanderkooi, J. M.; Owen, C. S.; Holtom, G. R.; Phillips, C. M. *Biophys. J.* **1990**, *58*, 177.  
 (57) Kaposi, A. D.; Vanderkooi, J. M. *Proc. Natl. Acad. Sci. U.S.A.* **1992**, *89*, 11371.  
 (58) Kaposi, A. D.; Fidy, J.; Stavrov, S. S.; Vanderkooi, J. M. *J. Phys. Chem.* **1993**, *97*, 6319.  
 (59) Broo, A.; Larsson, S. *Int. J. Quantum Chem.* **1989**, *16*, 185.  
 (60) Siddarth, P.; Marcus, R. A. *J. Phys. Chem.* **1993**, *97*, 6111.  
 (61) Mauk, M. R.; Mauk, A. G. *Biochemistry* **1982**, *21*, 4730.  
 (62) MacLachlan, S. J.; La Mar, G. N.; Sletten, E. *J. Am. Chem. Soc.* **1986**, *108*, 1285.  
 (63) Magner, E.; McLendon, G. *J. Phys. Chem.* **1989**, *93*, 7130.  
 (64) Milne, P. R.; Wells, J. R. E. *J. Biol. Chem.* **1970**, *245*, 1566.

Zinc mesoporphyrin IX diacid,<sup>50</sup> apomyoglobin,<sup>65,66</sup> and zinc myoglobin<sup>67</sup> were prepared, and zinc myoglobin was purified,<sup>50</sup> by published procedures. Zinc mesoporphyrin IX diacid and zinc myoglobin were always handled in the dark. This reconstituted protein, for which  $\epsilon_{414} = 2.5 \times 10^5 \text{ M}^{-1} \text{ cm}^{-1}$ , was quantitated spectrophotometrically. The absorbance quotient  $A_{414}/A_{280} = 17$  indicated high purity.

Distilled water was further demineralized to a resistance greater than 15 M $\Omega$ -cm. All the buffers were made with potassium phosphates of molecular biology grade. The stock buffer had a pH of 7.0 and an ionic strength of 10 mM; ionic strength was raised by addition of NaCl and lowered by dilution.

**Kinetics.** Laser kinetic spectroscopy (so-called laser flash photolysis) on the microsecond scale was done with a standard apparatus incorporating a Phase-R DL1100 laser and a methanol solution of rhodamine 590.<sup>29</sup> The absorbance-time curves were obtained and analyzed with software from OLIS, Inc. Sample solutions in a 10-mm cuvette were thoroughly deaerated by gentle flushing with ultrapure argon supplied by Air Products Co. Decay of the triplet-state  $^3\text{Zn}(\text{mb})$  was monitored at 460 nm, where this transient absorbance reaches a maximum. Appearance and disappearance of the cation radical  $\text{Zn}(\text{mb})^+$  were monitored at 675 nm, where the difference in absorbance between  $\text{Zn}(\text{mb})^+$  and  $^3\text{Zn}(\text{mb})$  is greatest. Each signal was an average of four (for the forward reaction) or ten (for the back reaction) pulses. The temperature was  $25 \pm 1^\circ\text{C}$ . The solid line in Figure 3b is a fit to eq 11, in which all absorbances ( $A$ ) are at 675

$$\Delta A(t) = \frac{k_9 A_{\text{cation}}}{k_{10} - k_9} [\exp(-k_9 t) - \exp(-k_{10} t)] + A_{\text{triplet}} \exp(-k_{\text{obs}} t) \quad (11)$$

nm,  $t$  is time,  $k_{\text{obs}}$  is the observed rate constant determined from the decay of  $^3\text{Zn}(\text{mb})$  monitored at 460 nm,  $k_9$  and  $k_{10}$  are the respective rate constants for appearance (eq 9) and disappearance (eq 10) of the cation radical  $\text{Zn}(\text{mb})^+$ ,  $A_{\text{triplet}}$  is the initial absorbance of  $^3\text{Zn}(\text{mb})$ , and  $A_{\text{cation}}$  is the maximum absorbance of  $\text{Zn}(\text{mb})^+$  in the absence of the back reaction (eq 10). This fitting can give a correct value of  $k_9$ , but it gives an incorrect value of  $k_{10}$  because the former process is of first order, whereas the latter one is of second order.

The concentration of zinc myoglobin was always 10  $\mu\text{M}$ . The concentrations of  $^3\text{Zn}(\text{mb})$  and  $\text{Zn}(\text{mb})^+$  depended on the excitation power used. The mole ratio of cupriplastocyanin to the triplet (eq 9) and of cupriplastocyanin to the cation radical (eq 10) was greater than 10:1. Each pseudo-first-order rate constant was an average result from repeated experiments, and second-order rate constants were obtained by least-squares fitting. The error bars in figures would have been smaller than the symbols for data points.

**Calculation of Dipole Moments.** Atomic coordinates for horse-heart myoglobin were obtained from its crystal structure.<sup>68</sup> Atomic coordinates for French-bean cupriplastocyanin were obtained from the crystal structure of the poplar protein<sup>10</sup> by replacing the relatively few nonhomologous amino acid residues. The iron(II) ion was replaced with a zinc(II) ion. Partial charges were assigned to all atoms.<sup>69,70</sup> The magnitude and orientation of the dipole moment were calculated by an established method.<sup>71,72</sup> It was reasonably assumed that at pH 7.0 lysine and arginine side chains and terminal amino groups are protonated and that carboxylic groups are deprotonated.

**Treatments of Electrostatic Interactions.** The dependence of reaction rates on ionic strength is commonly described in terms of Debye-Hückel theory, as in eq 12. The symbols  $k$  and  $k_0$  are bimolecular rate constants

$$\ln k = \ln k_0 - \frac{Z_1^2 \alpha \mu^{1/2}}{1 + \kappa R_1} - \frac{Z_2^2 \alpha \mu^{1/2}}{1 + \kappa R_2} + \frac{(Z_1 + Z_2)^2 \alpha \mu^{1/2}}{1 + \kappa R_*} \quad (12)$$

at ionic strengths  $\mu$  and zero;  $Z_1$  and  $Z_2$  are net charges of the reactants, and  $R_1$  and  $R_2$  are their radii;  $R_*$  is the radius of the transition state for the bimolecular reaction;  $\alpha = 1.17$  in water at  $25^\circ\text{C}$ ; and  $\kappa = 0.329 \mu^{1/2}$

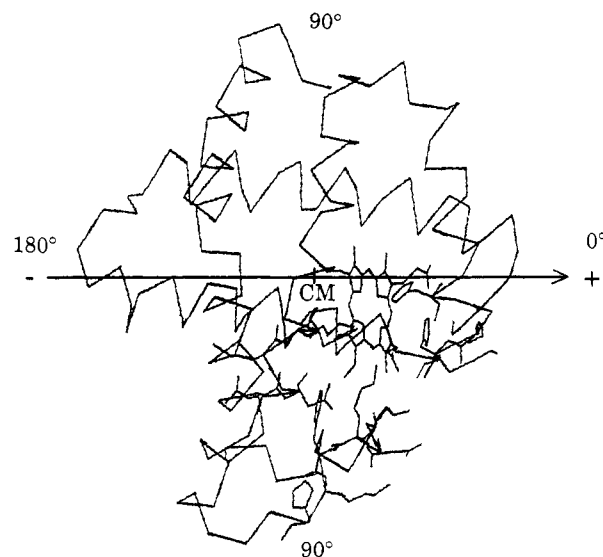


**Figure 1.** Chain of  $\alpha$ -carbon atoms and calculated dipole vector of ferromyoglobin. Angles  $\theta_2$  define positions with respect to the positive end of the dipole vector. The center of mass is marked CM.

$\text{\AA}^{-1}$ . Under the assumption  $R_1 = R_2 = R_{\text{av}}$ , eq 12 reduces to the widely-used eq 13, which is tested in this study. The radii of myoglobin and

$$\ln k = \ln k_0 + \frac{2Z_1 Z_2 \alpha \mu^{1/2}}{1 + \kappa R_{\text{av}}} \quad (13)$$

plastocyanin are 22 and 15.5  $\text{\AA}$ , respectively, and  $R_{\text{av}} = 22 \text{\AA}$  was used in the fittings.

The theory embodied in eq 14 recognizes not only net charges ( $Z$ ) but also dipole moments (vectors  $\mathbf{P}$  with magnitudes  $P$ ) of the protein molecules.<sup>73-76</sup> The monopole-dipole (eq 15) and dipole-dipole (eq 16) interactions are anisotropic—they depend on the location of the surface docking sites with respect to the dipole vectors. The function of ionic strength is defined in eq 17. The new symbols in eqs 14-17

$\ln k =$

$$\ln k_{\infty} - [Z_1 Z_2 + ZP(1 + \kappa R) + PP(1 + \kappa R)^2] \frac{e^2}{4\pi\epsilon_0\epsilon_k k_B T R} f(\kappa) \quad (14)$$

$$ZP = \frac{Z_1 P_2 \cos \theta_2 + Z_2 P_1 \cos \theta_1}{eR} \quad (15)$$

$$PP = \frac{P_1 P_2 \cos \theta_1 \cos \theta_2}{(eR)^2} \quad (16)$$

$$f(\kappa) = \frac{1 - \exp(-2\kappa R)}{2\kappa R_2 (1 + \kappa R_1)} \quad (17)$$

mean the following:  $\theta$  is the angle between the dipole vector and the vector from the center of mass (CM) to the reaction site on the surface (see Figures 1 and 2),  $R = R_1 + R_2$ ,  $\epsilon_0$  is the permittivity constant,  $\epsilon$  is the static dielectric constant,  $k_B$  is the Boltzmann constant, and  $e$  is elementary charge. Obviously, van Leeuwen theory can be applied only to proteins whose three-dimensional structure is known.

In eqs 12-17, subscript 1 designates plastocyanin and subscript 2 designates zinc myoglobin. Estimated uncertainty in  $\theta$  is the interval of its value over which the average difference between the best fitted and the experimentally determined values of  $k$  at all ionic strengths is 10% or less.

**The Mechanism.** A general mechanism for the redox reaction between the electron donor D and the electron acceptor A is shown in eq 18. The

(65) Teale, F. W. *Biochim. Biophys. Acta* **1959**, *35*, 543.

(66) Yonetani, T. *J. Biol. Chem.* **1967**, *242*, 5008.

(67) Leonard, J. J.; Yonetani, T.; Callis, J. B. *Biochemistry* **1974**, *13*, 1460.

(68) Evans, S. V.; Brayer, G. D. *J. Mol. Biol.* **1990**, *213*, 885.

(69) McCammon, J. A.; Wolynes, P. G.; Karplus, M. *Biochemistry* **1979**, *18*, 927.

(70) Northrup, S. H.; Pear, M. R.; Morgan, J. D.; McCammon, J. A.; Karplus, M. *J. Mol. Biol.* **1981**, *153*, 1087.

(71) Koppenol, W. H.; Margoliash, E. *J. Biol. Chem.* **1982**, *257*, 4426.

(72) Northrup, S. H.; Reynolds, J. C. L.; Miller, C. M.; Forrest, K. J.; Boles, J. O. *J. Am. Chem. Soc.* **1986**, *108*, 8162.

(73) van Leeuwen, J. W.; Mofers, F. J. M.; Veerman, E. C. I. *Biochim. Biophys. Acta* **1981**, *635*, 434.

(74) van Leeuwen, J. W. *Biochim. Biophys. Acta* **1983**, *743*, 408.

(75) Rush, J. D.; Lan, J.; Koppenol, W. H. *J. Am. Chem. Soc.* **1987**, *109*, 2679.

(76) Rush, J. D.; Levine, F.; Koppenol, W. H. *Biochemistry* **1988**, *27*, 5876.

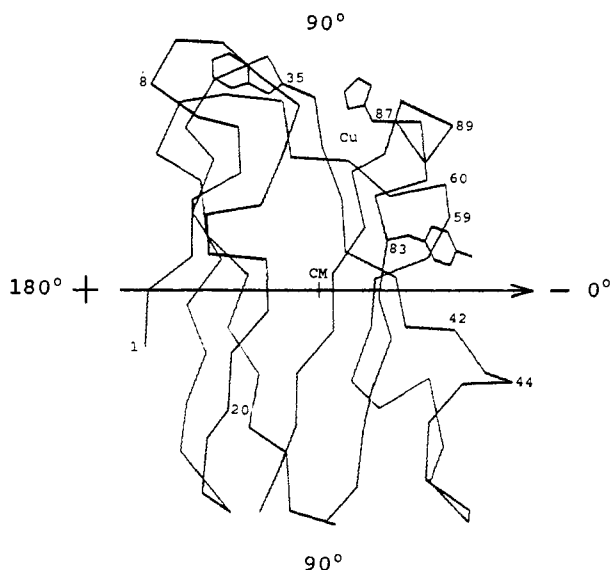
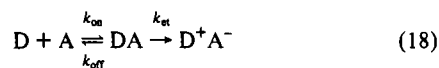


**Figure 2.** Chain of  $\alpha$ -carbon atoms and calculated dipole vector of cupriplastocyanin. The numerals represent selected amino acid residues, and angles  $\theta_1$  (see Table 2) define positions with respect to the negative end of the dipole vector. The center of mass is marked CM. Reprinted with permission from ref 29. Copyright 1993 American Chemical Society.



$$k_{\text{obs}} = \frac{k_{\text{et}}k_{\text{on}}[A]}{k_{\text{on}}[A] + k_{\text{off}} + k_{\text{et}}} \quad (19)$$

$$k_{\text{obs}} = K_A k_{\text{et}}[A] = k[A] \quad (20)$$

association constant  $K_A$  equals  $k_{\text{on}}/k_{\text{off}}$ . Under the steady-state approximation and the condition  $[A] \gg [D]$ , eq 19 is obtained.<sup>77</sup> In the limiting case when  $k_{\text{off}} > k_{\text{on}}[A]$ , eq 19 yields eq 20. In this limiting case, which is often invoked in studies of protein redox reactions, the observed rate constant linearly depends on the concentration of the reactant present in excess. The aforementioned treatments of electrostatic interactions apply only in this limiting case.

## Results

**Decay of  $^3\text{Zn}(\text{mb})$ .** The triplet excited state of both horseheart and sperm whale myoglobins decayed exponentially, with a rate constant of  $50 \pm 10 \text{ s}^{-1}$ , at concentrations from 10 to 100  $\mu\text{M}$  and over the entire range of ionic strength from 2.5 mM to 1.00 M. This rate constant remained unchanged in the presence of cupriplastocyanin, whose concentration was raised to 30  $\mu\text{M}$ .

**Forward Reaction, in Eq 9.** In the presence of cupriplastocyanin, decay of the triplet state became faster but remained exponential over the entire range of ionic strength. The rate constants for disappearance of  $^3\text{Zn}(\text{mb})$  (Figure 3a) and for appearance of  $\text{Zn}(\text{mb})^+$  (Figure 3b) were equal within the error bounds. As Figure 4 shows, the pseudo-first-order rate constant was linearly proportional to the cupriplastocyanin concentration, and it depended on ionic strength. Bimolecular rate constants, calculated from the slopes of the plots in Figure 4, are given in Table 1.

**Back Reaction, in Eq 10.** Addition of cupriplastocyanin in excess did not change the rate of  $^3\text{Zn}(\text{mb})$  quenching by cupriplastocyanin (eq 9), but it made the disappearance of  $\text{Zn}(\text{mb})^+$  (eq 10) a process of pseudo first order. The trace in Figure 3b is complicated because the back reaction occurs under second-order conditions. After pseudo-first-order conditions were established, the trace became exponential; see Figure 5. As Figure 6 shows, this pseudo-first-order rate constant was linearly

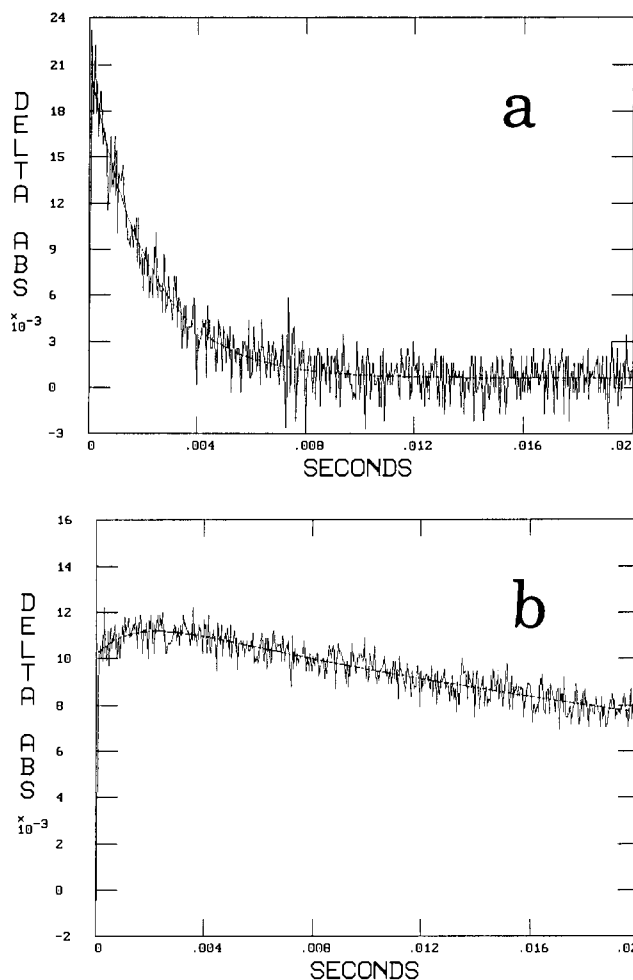


**Figure 3.** Transient absorbance in a solution containing 10  $\mu\text{M}$  zinc myoglobin and 30  $\mu\text{M}$  cupriplastocyanin in phosphate buffer at pH 7.0, ionic strength of 30 mM, and 25  $^{\circ}\text{C}$ . (a) Disappearance of the triplet state  $^3\text{Zn}(\text{mb})$ , monitored at 460 nm. The solid line is a single-exponential fit. (b) Appearance and slow disappearance of the cation radical,  $\text{Zn}(\text{mb})^+$ , monitored at 675 nm. The solid line is a fit to eq 11.

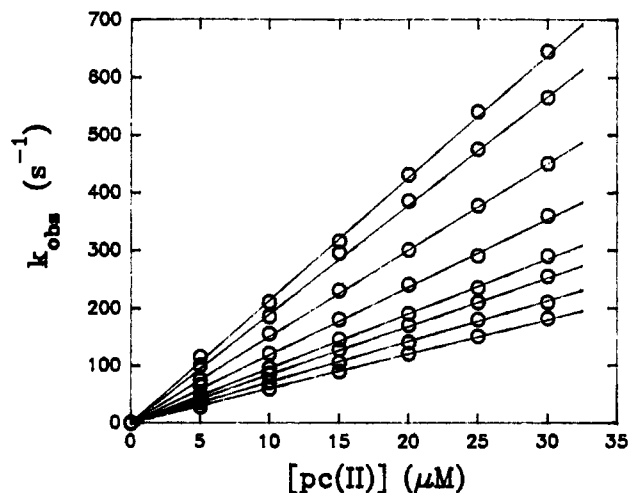


**Figure 4.** Rate of disappearance of the triplet-state  $^3\text{Zn}(\text{mb})$  in the forward reaction (eq 9) as a function of cupriplastocyanin concentration, in phosphate buffer at pH 7.0 and 25  $^{\circ}\text{C}$ . The solid lines are linear least-squares fits. Ionic strengths, from top to bottom: 2.5, 5.0, 10, 30, 100, 200, 500, and 1000 mM.

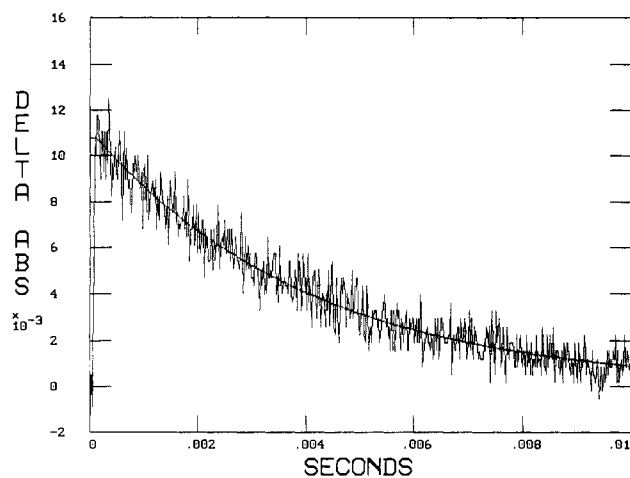
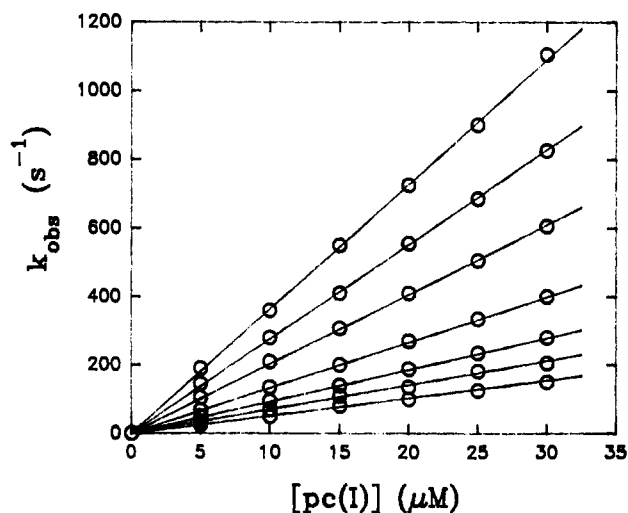
proportional to the cupriplastocyanin concentration, and it depended on ionic strength. Bimolecular rate constants, calculated from the slopes of the plots in Figure 6, are given in Table 1.

**Dipole Moments.** The net charge of native ferromyoglobin, derived from the protein composition, is zero in neutral solution.

(77) Strickland, S.; Palmer, G.; Massey, V. *J. Biol. Chem.* **1975**, *250*, 4048.

**Table 1.** Dependence on Ionic Strength of the Rate Constants ( $k \times 10^{-6} \text{ M}^{-1} \text{ s}^{-1}$ )<sup>a</sup> for Bimolecular Reactions at pH 7.0 and 25 °C

reaction	$\mu$ , mM							
	2.5	5.0	10	30	100	200	500	1000
forward, eq 9	21	19	15	12	9.4	8.3	7.2	5.9
back, eq 10		35	28	20	13	9.3	6.5	5.2

<sup>a</sup> Estimated error  $\pm 10\%$ .**Figure 5.** Transient absorbance at 675 nm of the cation radical  $\text{Zn}(\text{mb})^+$  in a solution containing 10  $\mu\text{M}$  zinc myoglobin, 30  $\mu\text{M}$  cupriplastocyanin, and 20  $\mu\text{M}$  cuproplastocyanin in phosphate buffer at pH 7.0, ionic strength of 1.00 M, and 25 °C. The solid line is a single-exponential fit.**Figure 6.** Rate of disappearance of the cation radical  $\text{Zn}(\text{mb})^+$  in the back reaction (eq 10) as a function of cuproplastocyanin concentration, in phosphate buffer at pH 7.0 and 25 °C. The solid lines are linear least-squares fits. Ionic strengths, from top to bottom: 5.0, 10, 30, 100, 200, 500, and 1000 mM.

The calculated dipole moment is 301 D, and it makes an angle of 44° with the normal to the average plane of the heme. We cautiously tried different plausible (de)protonation states of amino acid side chains and of the heme propionic groups. Although the magnitude of the dipole moment varied from 301 to 373 D, its orientation varied only from 44 to 52°. Therefore the angle  $\theta_2$ , which defines location of different protein parts, varied only within the error margins of the experiments and the fittings. The positive and negative ends of the dipole vector penetrate the protein surface near the  $\alpha$ -carbon atom of Ser92 and near the  $\alpha$ -carbon atom of Leu115, respectively. The entrance to the heme pocket is located at 20–80° with respect to the positive end of the dipole vector. The magnitude and orientation of the dipole moment in the native protein were assigned also to the protein derivative reconstituted with zinc(II).

**Table 2.** Orientations of Selected Sites in Horse-Heart Ferromyoglobin<sup>a</sup> with Respect to the Positive End of the Dipole Vector

site	$\theta_2$ , deg <sup>b</sup>	site	$\theta_2$ , deg <sup>b</sup>
Fe	29	His48	75–84
Lys45	51–71	His97	20–33
Lys47	56–77		

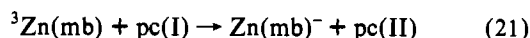
<sup>a</sup> These values are assigned also to the zinc(II) derivative of this protein.<sup>b</sup> Realistic positions of the  $\alpha$ -carbon atom in amino acid residues.**Table 3.** Orientations of Selected Sites in French-Bean Cupriplastocyanin with Respect to the Negative End of the Dipole Vector

patch	site	$\theta_1$ , deg
hydrophobic	Cu	80
	His87, imidazole	73–80
	Phe35, phenyl	107–110
acidic	Pro36, $\alpha$ -C	87
	Tyr83, ring	10–28
	cluster 42–45	18–42
	cluster 59–61	25–60

Cupriplastocyanin has a net charge of  $-8$  in neutral solution. The dipole moment is 362 D, and it makes an angle of 80° with the vector from the center of mass to the copper atom. The positive and negative ends of the dipole moment penetrate the protein surface near the  $\alpha$ -carbon atom of Glu2 and near the oxygen atom of Val41, respectively.<sup>29</sup> The locations of the reactive patches on the protein surface with respect to the dipole vector are given in Tables 2 and 3.

## Discussion

**Natural Decay of  $^3\text{Znmb}$ .** Zinc derivatives of both sperm whale and horse-heart myoglobins decay at the same rate, and our value of  $50 \pm 10 \text{ s}^{-1}$  is consistent with the values reported by others.<sup>37,50</sup> This value is independent of ionic strength and of zinc myoglobin concentration. The zinc derivative of the sperm whale protein (which is no longer readily available) was used only in these initial experiments, to verify our reconstitution procedures. All the kinetic experiments were done with the zinc derivative of the horse-heart protein, which is readily available. Because the decay rate (i.e., the lifetime) of the triplet state is unaffected by the presence of cuproplastocyanin, we conclude that reductive bimolecular quenching (eq 21) cannot compete with the natural decay under the experimental conditions used.



**The Forward Reaction.** Concomitant disappearance of the triplet state and appearance of the cation radical is evidence for redox quenching. Persistence of single-exponential decay of the triplet state and linearity of the plots in Figure 4 over the entire range of ionic strengths are evidence for a bimolecular reaction; see eq 9. Our previous studies<sup>25,30</sup> showed that  $^3\text{Zn}(\text{cyt})$  and  $^3\text{Sn}(\text{cyt})$  are quenched by cupriplastocyanin in both unimolecular (eqs 3 and 7) and bimolecular (eqs 4 and 8) reactions whose relative contributions varied smoothly with ionic strength because cytochrome *c* and plastocyanin electrostatically attract each other. The present study shows that  $^3\text{Zn}(\text{mb})$  is quenched solely in a bimolecular reaction because this electroneutral protein does not associate with plastocyanin in solution to the extent detectable in our kinetic experiments.

Cuproplastocyanin cannot be reduced further. Its addition to the reaction mixture does not affect the forward reaction because cuproplastocyanin can neither oxidatively quench  $^3\text{Zn}(\text{mb})$  nor successfully compete with the quencher (cupriplastocyanin) in interactions with zinc myoglobin.

**The Back Reaction.** The high concentration of cupriplastocyanin in these experiments ensured that the forward reaction (eq 9) was much faster than the subsequent back reaction (eq

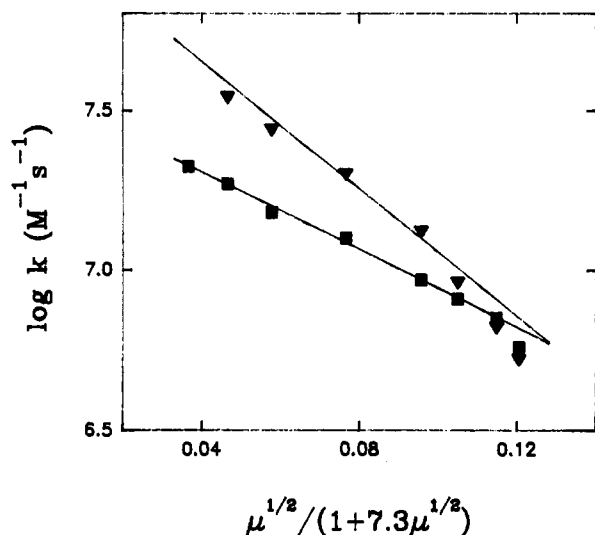


**Figure 7.** Fittings to eq 13 of the bimolecular rate constants in Table 1 for the forward (■) and back (▼) reactions, eqs 9 and 10, respectively. The rate constants at ionic strengths of 0.500 and 1.00 M were omitted from the fitting of the back reaction.

10). In this way the two reactions were separated in time, and interference between them was avoided. The linear plots in Figure 6 show that the back reaction, too, is purely bimolecular.

In terms of the mechanism in eqs 18–20, simple second-order kinetics that we found for both the forward (eq 9) and back (eq 10) reactions is evidence against a diprotein precursor complex. It should be kept in mind, however, that in a different limiting case, if complex formation and dissociation are faster than electron transfer within the complex, second-order kinetics would still be observed.

**Monopole–Monopole Electrostatic Interactions.** Although zinc myoglobin is electroneutral or nearly so at pH 7.0, Table 1 and Figure 4 show that the rate constant for the forward reaction (eq 9) decreases with increasing ionic strength as if this protein bore a positive charge. Clearly, there are electrostatic interactions other than monopole–monopole interactions between protein molecules. The back reaction (eq 10) depends on ionic strength more than the forward reaction (eq 9) does, and this small difference may be caused by a small positive charge of  $\text{Zn}(\text{mb})^+$ . At low and intermediate ionic strengths the back reaction is less than 2 times faster than the forward reaction, but at high ionic strengths, when electrostatic interactions are negligible, the rate constants for the two reactions become equal within the error margins.

Although Debye–Hückel theory does not strictly apply to macromolecules, it is often used to estimate charges of small, globular proteins. Fittings of the rate constants in Table 1 to eq 13 are shown in Figure 7. Fitting for the forward reaction (eq 9) over the entire range of ionic strength yielded a charge of +0.5 for zinc myoglobin. Fitting for the back reaction (eq 10) clearly failed at ionic strength greater than ca. 200 mM; when the fitting was limited to the range from 2.5 to 100 mM, the charge of +1.2 was obtained for the cation  $\text{Zn}(\text{mb})^+$ . These fittings to Debye–Hückel theory gave reasonable charges, but they did not advance our understanding of the electron-transfer reactions.

**Dipolar Interactions and Protein–Protein Orientation for Electron Transfer.** Because three-dimensional structures of myoglobin and of plastocyanin are known in detail, we were able to calculate their dipole moments and treat the kinetic results by van Leeuwen theory, embodied in eq 14. Because the charge (de)localization in the cation radical  $\text{Zn}(\text{mb})^+$  is uncertain, its dipole moment could not be calculated accurately. We refrained from fitting of the rate constants in Table 1 for the back reaction (eq 10) and fitted only those for the forward reaction (eq 9).

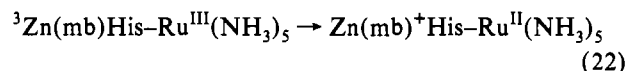
Dipolar interactions are an important, but sometimes neglected,

component of the total electrostatic interaction between macromolecules having asymmetric charge distributions. Dipolar interactions manifest themselves especially clearly when the reactants have large dipole moments and when the monopole–monopole interaction is weak because at least one of the reactants is electroneutral or nearly so. Dependence of the rate constant on ionic strength in this study (Table 1) and in some of the previous studies from this laboratory<sup>78,79</sup> is attributable mostly to dipolar interactions.

Although van Leeuwen theory (eq 14) is semiquantitative and applies best at low ionic strength,<sup>80</sup> it proved applicable also at intermediate and high ionic strengths.<sup>26,29,75,76,78,79,81–83</sup> The forward reaction (eq 9) should be suitable because, as discussed above, it occurs by a bimolecular mechanism. Most of the rate constants to be fitted here are obtained at ionic strengths of 100 mM and less, at which the theory is most valid. Dependence of reaction rates on ionic strength can be reproduced more rigorously in terms of Brownian dynamics, but these calculations are very demanding and approximations are often introduced to expedite them.<sup>80</sup> In a very recent study of electron-exchange reactions between metalloproteins, fitting with full-fledged Brownian dynamics theory was only slightly better than that with van Leeuwen theory.<sup>84</sup>

The quantities  $Z_1$ ,  $R_1$ , and  $P_1$  (for cupriplastocyanin) and  $Z_2$  and  $R_2$  (for zinc myoglobin) were constants in the fittings. The quantities  $P_2$  (for zinc myoglobin) and  $k_\infty$  were fixed parameters—changed from one fitting to another but kept constant during each fit. All the  $P_2$  values obtained for reasonable charge distributions (protonation states) of the protein were tried in the fittings. The choice of  $k_\infty$  was reliably guided by the trend in Table 1. The rate constant at infinite ionic strength is expected to be a little smaller than the known rate constant at the ionic strength of 1.00 M. We cautiously picked  $k_\infty$  values in a range that brackets the experimental value  $(5.9 \pm 0.6) \times 10^6 \text{ M}^{-1} \text{ s}^{-1}$ . The only variables in the fittings were the angles  $\theta_1$  and  $\theta_2$ , which define the locations of the sites in cupriplastocyanin and zinc myoglobin, respectively, with respect to the dipole vector in each protein. A typical result is shown in Figure 8. The solid line is the best fit to the rate constants. This and five other fits of good quality consistently gave the following results:  $\theta_1 = 98 \pm 15^\circ$  and  $\theta_2 = 60 \pm 11^\circ$ .

Although a  $\theta$  value defines a band, not a particular spot, on the protein surface, this value allows a distinction among distant areas on the surface. The fitted value of  $\theta_2$  is consistent with the location of the heme crevice and, more precisely, with an area near His48. Studies of the photoinduced reaction in eq 22 in four



derivatives of zinc myoglobin, each containing a  $\text{Ru}(\text{NH}_3)_5^{3+}$  tag at a different histidine residue, showed that the rate constant for the His48 derivative is nearly 1000 times greater than the rate constants for the other derivatives.<sup>53</sup> The reaction in eq 22 bears a similarity to the forward reaction in eq 9. Both the ruthenium complex and cupriplastocyanin seem to oxidize  ${}^3\text{Zn}(\text{mb})$  efficiently from the surface site at or near His48. Our finding and these previous findings consistently indicate that the area near His48 is favorable for electron transfer.

(78) Zhou, J. S.; Kostić, N. M. *Biochemistry* **1992**, *31*, 7543.

(79) Brothers, H. M., II; Zhou, J. S.; Kostić, N. M. *J. Inorg. Organomet. Polym.* **1993**, *3*, 59.

(80) Eltis, L. D.; Herbert, R. G.; Barker, P. D.; Mauk, A. G.; Northrup, S. H. *Biochemistry* **1991**, *30*, 3663.

(81) Dixon, D. W.; Hong, X.; Woehler, S. E. *Biophys. J.* **1989**, *56*, 339.

(82) Dixon, D. W.; Hong, X.; Woehler, S. E.; Mauk, A. G.; Sishta, B. P. *J. Am. Chem. Soc.* **1990**, *112*, 1082.

(83) Dixon, D. W.; Hong, X. *Adv. Chem. Ser.* **1990**, *226*, 162.

(84) Andrew, S. M.; Thomasson, K. A.; Northrup, S. H. *J. Am. Chem. Soc.* **1993**, *115*, 5516.

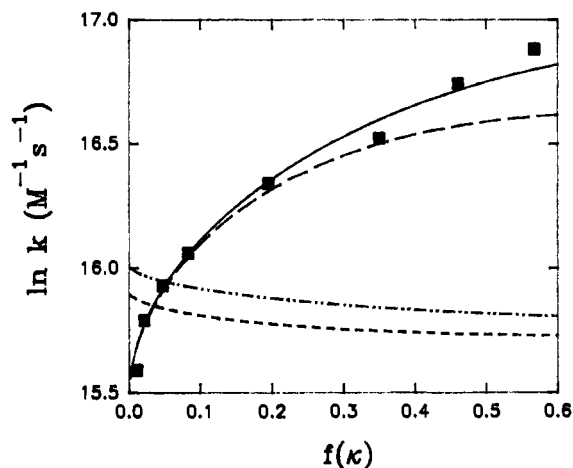
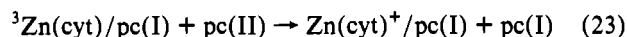


**Figure 8.** Fittings to eq 14 of the bimolecular rate constants in Table 1 (■) for the forward reaction, eq 9. In all fittings  $P_2 = 301$  D. The solid line is the best fit with the fixed parameter  $k_\infty = 6.0 \times 10^6 \text{ M}^{-1} \text{ s}^{-1}$ ; the results are  $\theta_1 = 98^\circ$  (hydrophobic patch) and  $\theta_2 = 60^\circ$  (heme crevice). The other lines are unsuccessful attempts at fitting with the following values for the parameters  $k_\infty$ ,  $\theta_1$ , and  $\theta_2$ , respectively: long dash,  $2.9 \times 10^6 \text{ M}^{-1} \text{ s}^{-1}$ ,  $30^\circ$  (acidic patch), and  $60^\circ$  (heme crevice); short dash,  $1.5 \times 10^7 \text{ M}^{-1} \text{ s}^{-1}$ ,  $30^\circ$  (acidic patch), and  $110^\circ$  (outside heme crevice); dash-dot-dot,  $8.9 \times 10^6 \text{ M}^{-1} \text{ s}^{-1}$ ,  $98^\circ$  (hydrophobic patch), and  $110^\circ$  (outside heme crevice).

As Table 3 shows, the value  $\theta_1 = 98 \pm 15^\circ$  is consistent with the hydrophobic patch, and inconsistent with the acidic patch, on the cupriplastocyanin surface. The broken lines in Figure 8 are attempted fits with a value of  $\theta_2$  corresponding to the reactive site on the zinc myoglobin surface outside of the heme crevice and with a value of  $\theta_1$  corresponding to the acidic patch on the cupriplastocyanin surface. These and other such attempts clearly failed. The difference between the successful and the unsuccessful fits in Figure 8 lies well outside the error margin of the measurements and the uncertainty of the fitting. We accept the finding that cupriplastocyanin uses its hydrophobic patch for the reaction in eq 9.

**Comparison with Other Reactions.** Because zinc cytochrome *c*, zinc myoglobin, and the covalent complex  $\text{Zn}(\text{cyt})/\text{pc}(\text{I})$  have similar redox potentials in the triplet state, the reactions in eqs 4, 9, and 23 all have a driving force of 1.2 eV. Zinc cytochrome



*c*, however, differs from the other two reductants in two respects. The first difference is in electrostatic properties. The positively charged patch on the surface of zinc cytochrome *c* is shielded by the negatively charged patch of cuproplastocyanin in the covalent complex  $\text{Zn}(\text{cyt})/\text{pc}(\text{I})$ ;<sup>34,78</sup> zinc myoglobin lacks distinct charged patches on the surface and bears no appreciable net charge. The second difference is in heme exposure. The partially exposed heme edge in zinc cytochrome *c* is largely covered by cuproplastocyanin in the covalent complex; the heme is buried in a crevice in zinc myoglobin. For reasons of both electrostatics and heme exposure, zinc myoglobin and  $\text{Zn}(\text{cyt})/\text{pc}(\text{I})$  are unlikely to reduce cupriplastocyanin from the acidic patch.

Although electrostatic interactions between myoglobin and plastocyanin are too weak to govern protein-protein orientation in the electron-transfer event, analysis of these interactions in terms of van Leeuwen theory gives information about this orientation. Analysis of dipolar interactions and comparison of the electrostatic and cross-linked complexes consistently indicated that cupriplastocyanin uses its acidic patch for the reaction in eq 4,<sup>25,26,29</sup> in which strong electrostatic interactions dominate the orientation. Analysis of dipolar interactions indicated that cupriplastocyanin uses its hydrophobic patch for the reactions in eqs 9 (this work) and 23,<sup>78</sup> in which electrostatic interactions are relatively weak and the dominant factor may be the need for optimal electronic coupling between the copper site and the buried zinc porphyrin. Protein-protein orientation does not seem to depend on the driving force for electron-transfer reaction.<sup>26</sup>

**Acknowledgment.** We thank the National Science Foundation for funding. N.M.K. thanks the A. P. Sloan Foundation for a Research Fellowship for 1991–1993.